Spectroscopy Identification and Thermodynamic Stability of *tert*-Butyl Nitrite and Methane Clathrate Hydrate

Boram Sung,[†] Kyuchul Shin,[†,‡] Minjun Cha,[†] Sukjeong Choi,[†] Jaehyoung Lee,[§] Yongwon Seo,[||] and Huen Lee*[,†]

Department of Chemical and Biomolecular Engineering (BK21 program) and Graduate School of EEWS, Korea Advanced Institute of Science and Technology (KAIST), 335 Gwahangno, Yuseong-gu, Daejeon 305-701, Korea Institute of Geoscience and Mineral Resources (KIGAM), 92 Gwahangno, Yuseong-gu, Daejeon 305-350, and Department of Chemical Engineering, Changwon National University, Changwon, Gyeongnam 641-773, Republic of Korea

Structure-H hydrate has been highlighted due to its higher gas storage capacity and favorable thermal stability. Here, we introduce a new structure-H hydrate former, *tert*-butyl nitrite, and identify it through spectroscopic analysis. The hydrate structure and guest distribution were examined by using powder X-ray diffraction, Raman spectroscopy, and solid-state high-power decoupling ^{13}C NMR spectroscopy. The phase equilibria ($L_w + H + L_g + V$) of *tert*-butyl nitrite + CH_4 hydrate were measured at pressures from (3 to 4.5) MPa and at temperatures from (277 to 282) K. We also investigated the kinetic behavior of this new high-polarity hydrate former.

Introduction

In contrast to sI and sII hydrates, which are generally stabilized by single occupants (guests), the sH structure requires two dissimilar guest molecules of different sizes to maintain its stability.[1] Large guest molecules (LGMs), such as 2,2-dimethylbutane (neohexane, NH),[2] methylcyclohexane (MCH),[3] methylcyclopentane, cyclooctane,[4] 2-methoxy-2-methylpropane (*tert*-butyl methyl ether, TBME),[5] and 1,1-dimethylcyclohexane (1,1-DMCH),[6] were identified as sH formers with small gaseous molecules (help gas). Recently, Susilo et al.[7] investigated whether the solubility of sH hydrate formers NH, MCH, and TBME in water could affect the hydrate formation kinetics. Particularly, TBME, having a higher solubility in water than NH and MCH, exhibits a faster rate of initial hydrate formation. The strong interaction between TBME and water also induced crystal growth to proceed slowly, causing the limited occupancy of methane molecules in the hydrate cages. The polarity of LGMs can result in hydrate structuring being quite complex.

In this study we measured the hydrate phase equilibria for a mixture containing gaseous methane and *tert*-butyl nitrite (TBN). Powder X-ray diffraction (PXRD), Raman spectroscopy, and solid-sate ^{13}C NMR spectroscopy were used to attain the analytical information on both the hydrate structure and guest distribution. We also attempted to examine the formation kinetics of NH and TBN hydrate with methane.

Experimental Section

Materials. CH_4 gas was purchased from Special Gas (Korea) with a stated minimum purity of 0.9995 mole fraction. TBN ($C_4H_9NO_2$; 0.9 mole fraction), NH (C_6H_{14}; 0.99 mole fraction), and TBME ($C_5H_{12}O$; 0.98 mole fraction) were supplied by Sigma-Aldrich, Inc. All chemicals were used without any further purification. Water of ultrahigh purity was obtained from a Millipore purification unit.

Methods. To measure the hydrate phase equilibria of the CH_4 [(3, 3.5, 4, and 4.5) MPa] + TBN (4.68 g, slightly in excess of 0.0286 mole fraction) + H_2O (25.0 g) sH samples, we followed the general procedures commonly adopted in the hydrate community.[5] First, the TBN solution was introduced into the equilibrium cell having a mechanical stirrer and a K-type thermocouple probe with a calibrated digital thermometer (Barnant 90) with an uncertainty of ± 0.05 K. A mechanical stirrer agitated the mixture containing solid hydrate crystals (keeping them dispersed uniformly) during the entire formation process. Second, the cell was immersed in a water−ethanol mixture bath, and its temperature was controlled by an externally circulating refrigerator/heater (Jeio Tech, RW-2025G) with an uncertainty of ± 0.05 K. The digital pressure gauge [DPI 104, (0 to 14) MPa] with 0.05 % full-scale accuracy was used to measure the system pressure. After being pressurized to a desired pressure with CH_4, the equilibrium cell was slowly cooled. When the system pressure drop had reached a steady state, the hydrate formation was considered to be complete. Then the equilibrium cell temperature was slowly elevated at a rate of 0.1 $K \cdot h^{-1}$ to dissociate the formed hydrate. The equilibrium point of the hydrate phase was determined by analyzing the pressure−temperature trace of hydrate formation and dissociation stages. For preparing a sample for spectroscopic analysis, the formed hydrate was finely ground in the liquid nitrogen vessel. PXRD patterns of the hydrate sample (ground to a fine powder of ~200 μm) were recorded at 93.15 K on a Rigaku D/MAX-2500 device using a light source and graphite-monochromatized Cu Kα_1 radiation with a wavelength of 1.5406 Å in the $\theta/2\theta$ scan mode. The PXRD experiments were carried out in step mode with a fixed time of 3 s and a step size of 0.02° for $2\theta = 5°$ to 55°. Raman measurements were performed using a LabRAM HR UV/vis/NIR instrument at 93.15 K using the focused 514.53 nm line of an Ar ion laser for excitation. The laser intensity was typically 25 mW. The scattered light

* Corresponding author. Fax: +82-42-350-3910. Phone: +82-42-350-3917. E-mail: h_lee@kaist.ac.kr.
[†] KAIST.
[‡] Current address: National Research Council of Canada, 100 Sussex Dr., Ottawa K1A 0R6, Canada.
[§] KIGAM.
[||] Changwon National University.

10.1021/je100966g
Published on Web 11/24/2010

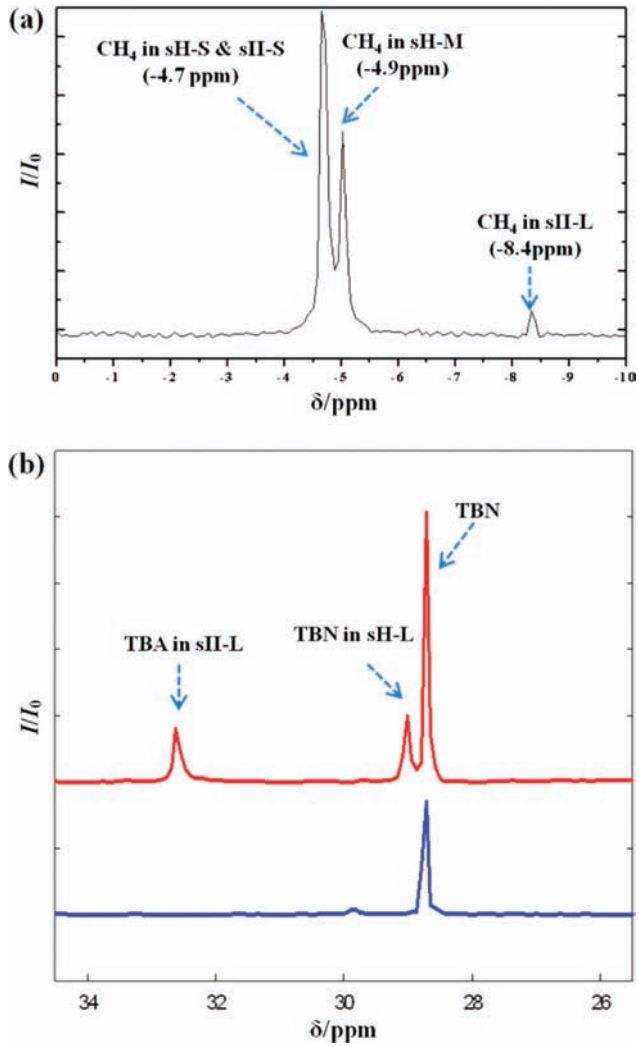

Figure 1. HPDEC ^{13}C NMR spectra of (a) TBN + CH_4 + H_2O clathrate hydrate in the range from (0 to −10) ppm and (b) TBN + CH_4 + H_2O clathrate hydrate (red line) and TBN + ice powder sample (blue line) in the range from (25.5 to 34.5) ppm (I/I_0, relative NMR intensity; δ, chemical shift).

was dispersed using a single-grating spectrometer and detected with a electrically cooled (−70 °C) CCD detector. A Bruker (Billerica, MA) AVANCE 400 MHz solid-state NMR spectrometer was used in this study. The powdered samples were placed in a 4 mm o.d. zirconia rotor loaded into a variable-temperature probe. All ^{13}C NMR spectra were recorded at a Larmor frequency of 100.6 MHz with magic angle spinning (MAS) at approximately 5 kHz. A pulse length of 2 μs and a pulse repetition delay of 5 s under proton decoupling were employed with a radio frequency field strength of 50 kHz, corresponding to 5 μs 90° pulses. The downfield carbon resonance peak of adamantane, assigned as a chemical shift of 38.3 ppm at 300 K, was used as an external chemical shift reference. To find the early stage of hydrate formation kinetics of NH and TBN with CH_4 hydrate, an agitated kinetic apparatus was operated at constant temperature and pressure. The reactor vessel was pressurized at 303 K. After the temperature and pressure in the reactor were stabilized, the temperature of the alcohol bath was lowered to 275 K at 0.42 K·min^{-1}. The pressure was continuously recorded to find the induction time, which was the time period just before a sudden pressure drop was observed. The suitable period for hydrate crystal nucleation and growth was also checked at the constant temperature and pressure conditions of 275 K and 5 MPa.

Results and Discussion

Spectroscopic Identification of TBN + CH_4 Hydrate. First, the TBN + CH_4 hydrate sample was identified by high-power decoupling (HPDEC) ^{13}C NMR spectroscopy. Figure 1a shows the distribution of CH_4 guest molecules in the TBN + CH_4 hydrate, representing CH_4 in a small 5^{12} cage (sH-S and sII-S; $\delta_C = -4.7$ ppm) and a middle $4^3 5^6 6^3$ cage (sH-M; $\delta_C = -4.9$ ppm) of the sH hydrate. The area ratio of two representative sH−CH_4 peaks ($A_{sH\text{-}S}/A_{sH\text{-}M}$) is identified to be approximately 1.5; this result shows good agreement with that of the common sH hydrate.[1] A small additional peak at $\delta_C = -8.4$ ppm (large $5^{12}6^4$ cage, sII-L) indicates that sII-CH_4 hydrate also coexists in this sample. Additional formation of sII hydrate originated from an impurity of TBN (0.9 mole fraction purity of TBN) solution; 0.1 mole fraction of 2-methylpropan-2-ol (*tert*-butyl alcohol, TBA) as an impurity forms the sII hydrate with CH_4.[8] In Figure 1b, we observe the encaged TBN in the sH-L cage and encaged TBA in sII-L. The structure of TBN + CH_4 hydrate was also checked by PXRD as shown in Figure 2. The PXRD pattern of TBN + CH_4 hydrate clearly shows some ice and sII

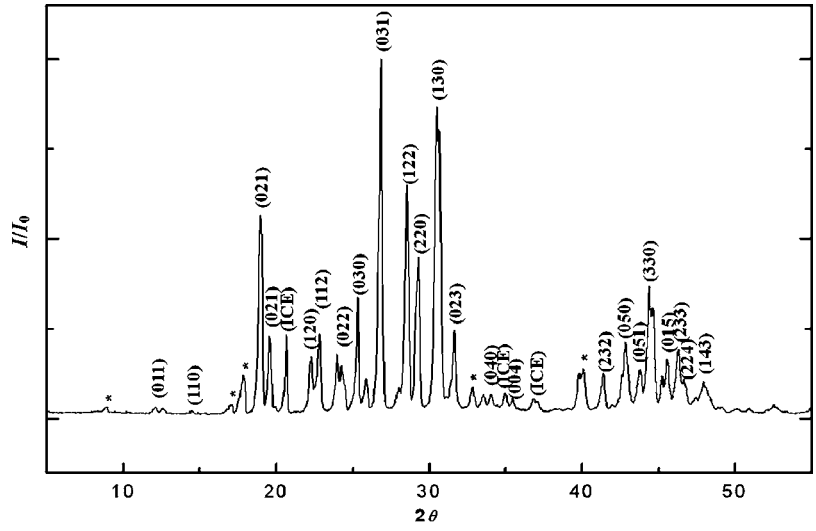

Figure 2. PXRD pattern of the TBN + CH_4 + H_2O clathrate hydrate (I/I_0, relative XRD intensity). The diffraction peaks of hexagonal ice are indicated by "(ICE)", and the peaks of the sII hydrate as an impurity are indicated by asterisks.

Table 1. Miller Indices of TBN + CH_4 + H_2O Clathrate Hydrate

h k l	*d*(exptl)	*d*(calcd)	*d*(exptl − calcd)
0 1 1	7.3026	7.2952	0.0074
1 1 0	6.0872	6.0723	0.0149
0 2 1	4.6793	4.6617	0.0176
0 2 1	4.6429	4.6671	−0.0242
1 2 0	3.9922	3.9752	0.017
1 1 2	3.8988	3.8889	0.0099
0 2 2	3.6658	3.6476	0.0182
0 3 0	3.512	3.5058	0.0062
0 3 1	3.3154	3.3129	0.0025
1 2 2	3.124	3.1268	−0.0028
2 2 0	3.0457	3.0361	0.0096
1 3 0	2.9286	2.917	0.0116
0 2 3	2.8282	2.8408	−0.0126
0 4 0	2.6317	2.6294	0.0023
0 0 4	2.5301	2.5318	−0.0017
2 3 2	2.1797	2.1782	0.0015
0 5 0	2.1097	2.1035	0.0062
0 5 1	2.0657	2.0595	0.0062
3 3 0	2.03	2.0241	0.0059
0 1 5	1.9911	1.9889	0.0022
2 3 3	1.9594	1.963	−0.0036
2 2 4	1.9447	1.9445	0.0002
1 4 3	1.8965	1.8901	0.0064

hydrate peaks due to the impurity of the TBN solution. The structure and lattice parameters of TBN + CH_4 hydrate were checked by the Checkcell program (Laugier),[9] and the structure was identified to be hexagonal (space group *P*6/*mmm*) with lattice parameters of $a = (1.2145 \pm 0.0020)$ nm and $c = (1.0127 \pm 0.0059)$ nm. All the refined values are in good agreement with the literature values of $a = 1.22$ nm and $c = 1.01$ nm for the sH hydrate.[1,10] Table 1 presents the Miller indices of TBN + CH_4 hydrate. Raman spectroscopy was used to further confirm the incorporation of methane molecules in the hydrate cavities. The Raman spectra for the TBN + CH_4 hydrate and TBN + H_2O mixed ice powder samples for reference are shown in Figures 3 and 4. In Figure 4b, the peak around 2913 cm^{-1} represents the C−H stretching vibrational mode of the CH_4 molecule in the sH hydrate. Two peaks at around (1611 and 810) cm^{-1} represent the N═O stretching and O−N stretching modes of TBN, respectively. The C−O stretching mode peaks are observed at around (1190 and 950) cm^{-1}. The O−N═O stretching mode of TBN is also detected at around 580 cm^{-1}.[10]

Hydrate Phase Equilibria for sH TBN + CH_4 + H_2O. The $L_w + L_g + H + V$ four-phase equilibrium data of TBN + CH_4 hydrate were measured at pressures from (3 to 4.5) MPa and at temperatures from (277 to 282) K. The equilibrium data sets are plotted in Figure 5 and listed in Table 2. In Figure 5, other literature phase equilibrium data of pure CH_4, NH + CH_4, and TBME + CH_4 hydrate systems are also plotted. The thermodynamic stability of TBN + CH_4 hydrate is higher than that of pure CH_4 hydrate at pressures from (3 to 4.5) MPa and at temperatures from (277 to 282) K.

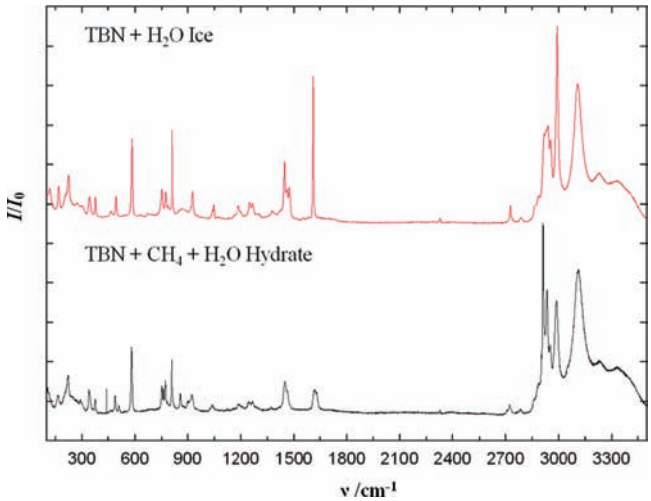

Figure 3. Raman spectra of TBN + CH_4 + H_2O clathrate hydrate and TBN + H_2O ice in the range of (0 to 3500) cm^{-1} (I/I_0, relative Raman intensity; ν, Raman shift).

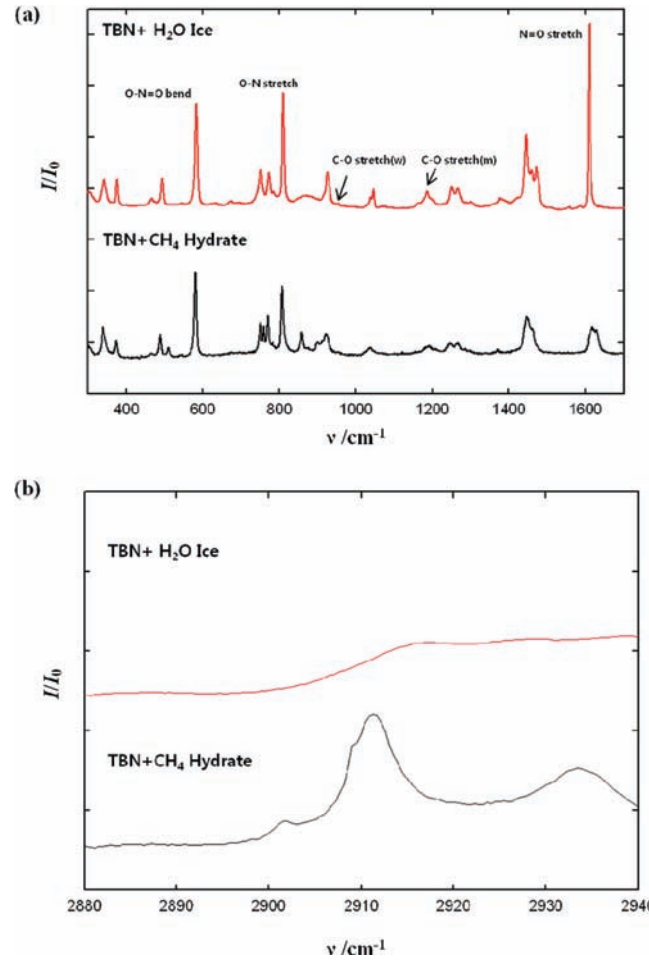

Figure 4. Raman spectra of TBN + CH_4 + H_2O clathrate hydrate and TBN + H_2O ice at 203.15 K in the ranges of (a) (300 to 1700) cm^{-1} and (b) (2880 to 2940) cm^{-1} (I/I_0, relative Raman intensity; ν, Raman shift).

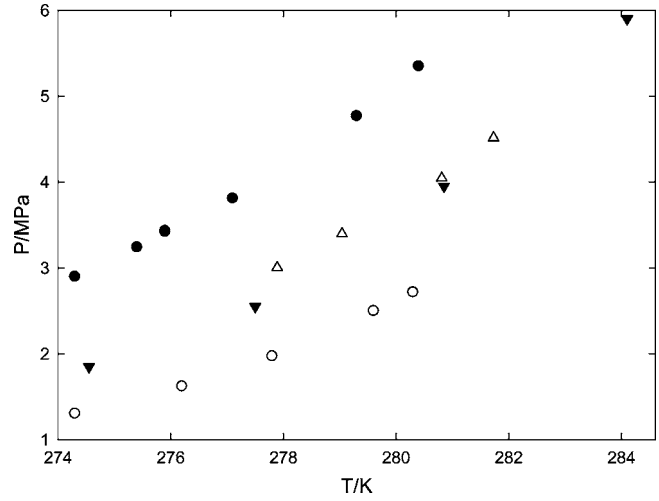

Figure 5. Pressure−temperature diagram for NH + CH_4, TBME + CH_4, TBN + CH_4, and pure CH_4 hydrate: ○, NH + CH_4 hydrate;[11] ▼, TBME + CH_4 hydrate;[12] ●, pure CH_4 hydrate;[13] △, TBN + CH_4 hydrate.

Table 2. Four-Phase (L_w + H + L_g + V) Equilibria of the TBN + CH_4 + Water System

T / K	P / MPa	T / K	P / MPa
277.89	3.00	280.81	4.04
279.04	3.39	281.73	4.51

Kinetic Behavior of TBN + CH_4 Hydrate and NH + CH_4 Hydrate. The effect of polar LGMs on the hydrate formation kinetics was divided into two stages of nucleation and growth for forming sH crystals. We first attempted to compare the kinetic rate difference between polar TBN and nonpolar NH. Both sH formers with the aid of a second guest (CH_4) participated in the corresponding sH hydrates. In Figure 6, the induction time, 3600 s, of sH TBN + CH_4 is much faster than that, 14000 s, of sH NH + CH_4. The hydrate inductions behave in a stochastic manner and largely depend on a variety of external variables. In this regard, we tried to check several times for each kinetic induction data set and observed the consistent induction tendency for both TBN + CH_4 and NH + CH_4 hydrates. On the other hand, during hydrate crystal growth, the system was maintained at 5 MPa and 275 K. Even when the cell pressure continued to decrease, the hydrate crystals continued to grow. The pressure vs time curve in Figure 7 indicates that both the hydrate conversion and CH_4 capacity (CH_4 occupancy in sH-S and sH-M) for the TBN + CH_4 system are much lower than those of the NH + CH_4 system, although the mole fractions of TBN and NH in the water solution are the same. One plausible explanation is that the TBN has much more polarity in water and wets ice much better than NH at the initial stage (polarity of TBN, 2.8827 D; polarity of NH, 0.064 D),[14] leading to faster induction of TBN + CH_4. In contrast, during crystal growth, the relatively strong interaction between TBN and water molecules interrupts hydrate crystallization. This rather rough description needs to be confirmed again through more accurate and reliable kinetic experiments.

Conclusions

In this study, we identified a new structure-H hydrate former, *tert*-butyl nitrite, by using powder X-ray diffraction, Raman spectroscopy, and solid-state high-power decoupling ^{13}C NMR spectroscopy. From the results of hydrate equilibrium measurement, it was found that TBN + CH_4 hydrate is more stable than pure CH_4 hydrate at pressures from (3 to 4.5) MPa and at temperatures from (277 to 282) K. The kinetic data suggest that the new hydrate former promotes the nucleation process, maybe due to its high polarity, but during hydrate growth, the polar interaction between TBN and water molecules may inhibit hydrate crystallization.

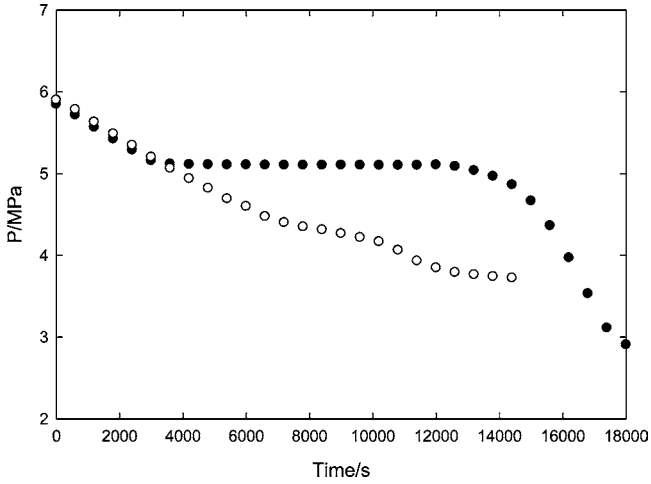

Figure 6. Pressure−time curve of TBN + CH_4 and NH + CH_4 hydrates with a change of temperature from (303 to 275) K: ●, NH + CH_4 hydrate; ○, TBN + CH_4 hydrate.

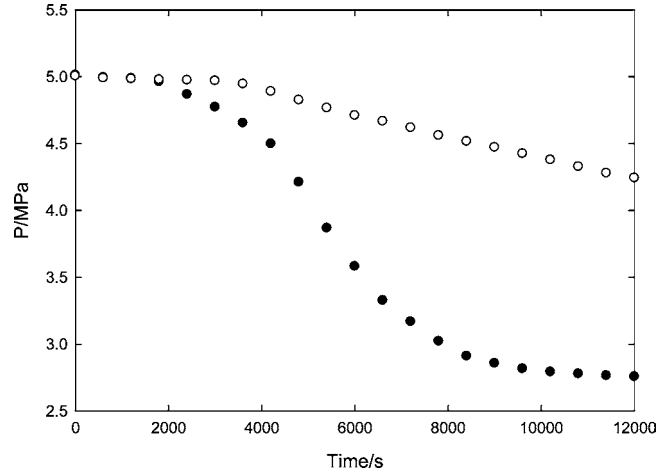

Figure 7. Pressure−time curve of TBN + CH_4 and NH + CH_4 hydrates with a constant temperature of 275 K: ●, NH + CH_4 hydrate; ○, TBN + CH_4 hydrate.

Literature Cited

(1) Sloan, E. D.; Koh, C. A. *Clathrate Hydrates of Natural Gasese*, 3rd ed.; CRC Press: Boca Raton, FL, 2008.
(2) Mehta, A. P.; Sloan, E. D. *J. Chem. Eng. Data* **1993**, *38*, 580–582.
(3) Mehta, A. P.; Sloan, E. D. *AIChE J.* **1994**, *40*, 312–320.
(4) Makino, T.; Nakamura, T.; Sugahara, T.; Ohgaki, K. *Fluid Phase Equilib.* **2004**, *218*, 235–238.
(5) Ohgaki, K.; Makihara, Y.; Takano, K. *J. Chem. Eng. Jpn.* **1993**, *26*, 558–564.
(6) Sugahara, T.; Hara, T.; Hashimoto, S.; Ohgaki, K. *Chem. Eng. Sci.* **2005**, *60*, 1783–1786.
(7) Susilo, R.; Alavi, S.; Lang, S.; Ripmeester, J.; Englezos, P. *J. Phys. Chem. C* **2008**, *112*, 9106–9113.
(8) Park, Y.; Cha, M.; Shin, W.; Lee, H.; Ripmeester, J. A. *J. Phys. Chem. B* **2008**, *112*, 8443–8446.
(9) Laugier, J.; Bochu, B. (Laboratorire des Materiaus et du Genie Physique, Ecole Superieure de Physique de Grenble). http://www.ccp14.ac.uk.
(10) McLaughlin, R. P.; Donald, W. A.; Jitjai, D.; Zhang, Y. *Spectrochim. Acta* **2007**, *67A*, 178–187.
(11) Ohmura, R.; Uchida, T.; Takeya, S.; Nagao, J.; Minagawa, H.; Ebinuma, T.; Narita, H. *J. Chem. Eng. Data* **2003**, *48*, 1337–1340.
(12) Hutz, U.; Englezos, P. *Fluid Phase Equilib.* **1996**, *117*, 178–185.
(13) Deaton, W. M.; Frost, E. M., Jr. *U.S. Bur. Mines Monogr.* **1946**, *8*, 101.
(14) The polarity values of TBN and NH were calculated by geometry optimization (WebMO program, http://www.webmo.net/index.html) with B3LYP/6-311+G(d,p).

Received for review September 27, 2010. Accepted November 9, 2010. We acknowledge funding from the Ministry of Knowledge Economy through the Recovery/Production of Natural Gas Hydrate Using Swapping Technique (KIGAM-Gas Hydrate R&D Organization). This work was also supported by National Research Foundation of Korea (NRF) grants [Leading Research Support Program, 2010-0029176; WCU program, R31-2008-000-10055-0] funded by the Ministry of Education, Science and Technology (MEST).

JE100966G